FULL PAPER

Dalton
www.rsc.org/dalton

Crystal structures of metal–organic frameworks sustained by π–π interactions between triple-helices

Mo Hong, Fang Chen-jie, Duan Chun-ying,* Li Yu-ting and Meng Qing-jin
Coordination Chemistry Institute, the State Key Laboratory of Coordination Chemistry, Nanjing University, Nanjing 210093, P. R. China. E-mail: duancy@nju.edu.cn

Received 25th September 2002, Accepted 30th January 2003
First published as an Advance Article on the web 27th February 2003

Metal–organic frameworks $[(Fe_2L_3)\cdot(C_4H_{10}O)]$ **1**, $[(Fe_2L_3)\cdot(C_5H_5N)]$ (**2**), $[(Fe_2L_3)\cdot(C_6H_6)]$ (**3**) and $[(Fe_2L_3)\cdot(C_4H_8O)_4]$ (**4**), achieved from triple metal helical iron complex $\mathbf{Fe_2L_3}$, were assembled in the solvents of diethyl ether/DMF, pyridine, benzene and THF, respectively, where $\mathbf{H_2L}$ is one of the simplest imine-based ligands $\{[(C_6H_4)(OH)]CH{=}N{-}N{=}CH[(OH)(C_6H_4)]\}$. Compounds **1**, **2**, **3** and **4** all crystallize in a centro-symmetric space group, consequently the molecules occur as a racemic mixture of Δ–Δ and Λ–Λ configuration enantiomers, wherein the equivalent fragments are related by the C_2 axis. The phenyl rings of the helical units contact the neighbors *via* π–π (face-to-face) and C–H ··· π interactions to form two-dimensional channeled frameworks in which solvent molecules are absorbed in the channels in each of the structures. Thermogravimetric analyses reveal that the solvent molecules can be evacuated from the pores without loss of the framework periodicity. The crystal lattice is thermally stable up to 350 °C, and diethyl ether can be re-adsorbed by putting the heated material in diethyl ether solvent. It is also interesting to find that upon addition of other solvents such as *n*-hexane and cyclohexane, thermal gravimetric measurement and elemental microanalysis do not support the absorbance of these guests, indicating that the inclusion can be selectively re-absorbed. All the results indicate that although C–H ··· π interactions have energies that are only in the range of 2–20 kJ mol^{-1}, these interactions are significant enough in combination that the orientation of molecules in the solid can be predicted with a reasonable degree of accuracy.

Introduction

Interactions between aromatic molecules present an important class of intermolecular force in chemistry, biology, materials science and crystallography.[1–3] It is generally recognized that,[4,5] in the absence of strong hydrogen-bond donors and acceptors, aromatic compounds tend to self-assemble *via* π–π (face–face) interactions, C–H ··· π interactions (T-shape geometry, edge–face or herringbone interactions) or both, and these weak non-covalent bonds can sustain supramolecular synthons which are structure determining.[6–10] Examples illustrating the importance and diversity of these interactions include the base pair association that stabilizes the double helical structure of DNA,[11] the tertiary structures of proteins,[12] packing of aromatic molecules in crystals,[5] host–guest bonding *etc.*[13] Previous studies generally focused on the use of organic compounds,[14,15] while in our assembly of porous-like frameworks,[16] we have introduced newly triple helices $\mathbf{Fe_2L'_3}$ to interact with each other, thereby offering the potential of broadening the scope of further work in this area. The ligand $\mathbf{H_2L'}$ (Scheme 1) used to assemble the triple helicate is one of the simplest imine-based ligands.[17,18] The ease of synthesis of these ligand systems has allowed to systematic probing of the effects of modifications to the ligand backbone through which the precise topography or macroarchitecture of the arrays should be controlled.

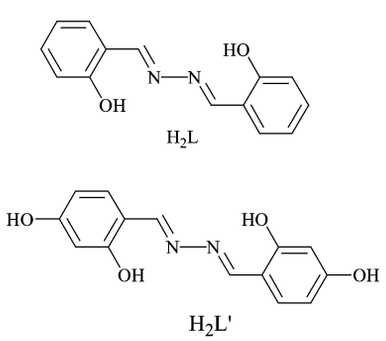

Scheme 1

The goal of crystal engineering is to recognize and design synthons that are robust enough to be exchanged from one network to another, which ensures generality and predictability. Such structural predictability leads to the anticipation of one, two and three dimensional patterns formed *via* intermolecular interactions.[19–21] It is suggested[22] that although the weak C–H ··· π interactions have energies only in the range of 2–20 kJ mol^{-1}, such interactions still be important for transient processes such as those associated with biomolecular structure and conformation, and their effects on crystal structure and packing are just as predictable as the effects of conventional hydrogen bonding and strong π–π stacking interactions. To continuously study the potential factors influencing the molecular packing of such helices, here we have prepared novel compounds of helical structure to construct the framework $\mathbf{Fe_2L_3}$ (Scheme 1) and study the influences of solvent on the crystallization. Thermo-gravimetric analyses were also carried out to study the thermal stability of such porous materials.

Experimental

General

All chemicals were of reagent grade quality obtained from commercial sources and used without further purification. Elemental analyses (C, H, and N) were carried out on a Perkin-Elmer 240 analyzer. X-Ray powder diffraction patterns were recorded on a D/max-γ A rotating anode X-ray diffractometer with graphite-monochromatic Cu-Kα (mean λ *ca.* 1.542 Å) radiation at room temperature. Differential thermal analysis and thermogravimetric analysis (DTA–TGA) were conducted on a TA Instruments SDT 2960 simultaneous DTA-TGA in a nitrogen atmosphere at a heating rate of 5 °C min^{-1}.

Preparation of compounds 1–4

The ligand $\mathbf{H_2L}$ was prepared according to the literature method.[16] The triple-helical iron complex $\mathbf{Fe_2L_3}$ was synthesized by simply refluxing the mixture of $\mathbf{H_2L}$ (0.63 g, 3 mmol) and $Fe(NO_3)_3\cdot 9H_2O$ (1.2 g, 3 mmol) in 25 mL methanol for 4 h.

DOI: 10.1039/b209366a

Table 1 Crystallographic data for compounds **1**–**4**

	1	**2**	**3**	**4**
Molecular formula	$C_{46}H_{42}Fe_2N_6O_7$	$C_{47}H_{37}Fe_2N_7O_6$	$C_{48}H_{38}Fe_2N_6O_6$	$C_{58}H_{64}Fe_2N_6O_{10}$
M	902.57	907.54	906.56	1116.87
Crystal system	Orthorhombic	Orthorhombic	Orthorhombic	Orthorhombic
Space group	*Pnna*	*Pnna*	*Pnna*	*Pbcn*
a/ Å	19.446(4)	19.557(4)	19.567(4)	15.165(3)
b/ Å	16.670(3)	16.232(3)	16.291(3)	19.115(3)
c/ Å	14.582(3)	14.405(3)	14.430(3)	18.888(3)
U/ Å^3	4727.0(16)	4572.9(16)	4599.8(16)	5475.3(17)
Z	4	4		4
T/K	293(2)	293(2)		293(2)
μ/mm^{-1}	0.667	0.689		0.594
No. reflections measured	79832	4189		4830
No. unique reflections (R_{int})	5506 (0.101)	4020 (0.001)		3191 (0.058)
R_1	0.056	0.053		0.047
wR_2	0.151	0.171		0.120

Dark-brown solid formed was isolated by filter, washed with methanol and dried over P_2O_5 under vacuum. Yield: 91%. Dark- brown crystals of **1** [$(Fe_2L_3)\cdot(C_4H_{10}O)$] were obtained by slow diffusion of diethyl ether into a chloroform solution. Found for **1**: C, 60.8; H, 4.6; N, 9.1; calc. for $[C_{42}H_{32}N_6O_6Fe_2]\cdot(C_4H_{10}O)$: C, 61.2; H, 4.7; N, 9.3%. IR (cm^{-1}, KBr disk): 3052 (ν_{C-H}), 2863, 1610, 1580, 1478, 1449 ($\nu_{C=C}$, $\nu_{C=N}$), 1271 (ν_{N-N}), 1098, 623 (ν_{Cl-O}), 753 (ν_{C-H}). Dark-brown crystals of **2** [$(Fe_2L_3)\cdot(C_5H_5N)$] were obtained by slowly evaporating a pyridine solution in air. Found for **2**: C, 61.9; H, 4.0; N, 11.2; calc. for $[C_{42}H_{32}N_6O_6Fe_2]\cdot(C_5H_5N)$: C, 62.2; H, 4.1; N, 10.8%. Dark-brown crystals of **3** [$(Fe_2L_3)\cdot(C_6H_6)$] were obtained by slowly evaporating a benzene solution in air. Found for **3**: C, 63.2; H, 4.7; N, 9.7; calc. for $[C_{42}H_{32}N_6O_6Fe_2]\cdot(C_6H_6)$: C, 63.6; H, 4.2; N, 9.3%. Dark-brown crystals of **4** [$(Fe_2L_3)\cdot(C_4H_8O)_4$] were obtained by slowly evaporating a THF solution in air. Found for **4**: C, 62.9; H, 5.7; N, 7.7; calc. for $[C_{42}H_{32}N_6O_6Fe_2]\cdot(C_4H_8O)_4$: C, 62.4; H, 5.8; N, 7.5%.

Preparation of compounds 5–8

Material **5** was synthesized by heating compound **1** up to 280 °C for 24 h. Found: C, 61.2; H, 3.7; N, 10.2; calc. for $C_{42}H_{32}N_6O_6Fe_2$: C, 60.9; H, 3.9; N, 10.1%. Putting material **5** (10 mg) in 1 mL diethyl ether–cyclohexane (1 : 10/v : v) for 24 h obtains material **6**. Found: C, 61.4; H, 4.4; N, 9.3; calc. for $[C_{42}H_{32}N_6O_6Fe_2]\cdot(C_4H_{10}O)$: C, 61.3; H, 4.5; N, 9.3%. Materials of **7** and **8** were obtained by putting material **5** (10 mg) in 1 mL *n*-hexane and cyclohexane, respectively, for 24 h. Found for **7** and **8**: C, 61.0; H, 3.9; N, 10.0; and C, 61.2; H, 4.5; N, 9.9; calc. for $C_{42}H_{32}N_6O_6Fe_2$: C, 60.9; H, 3.9; N, 10.1%.

Crystallography

Parameters for data collection and refinement of compounds **1**–**4** are summarized in Table 1. Selected bond distances and angles are listed in Table 2. Intensities of complexes **1** and **4** were collected on a Siemens SMART-CCD diffractometer with graphite-monochromatic Mo-Kα radiation (λ = 0.71073 Å) using the SMART and SAINT programs.[23] Intensities of complex **2** were collected on a Siemens P4 diffractometer with graphite-monochromatic Mo-Kα radiation (λ = 0.71073 Å) using the XSCANS program.[24] The structures were solved by direct methods and refined on F^2 using full-matrix least-squares methods using SHELXTL version 5.1.[25] The absorbed diethyl ether, pyridine and THF were refined as being disordered. For diethyl ether, the site occupancy factors for C(22), C(23), C(24) and C(25) were fixed at 0.76, 0.38, 0.38 and 0.38, respectively; for C(24′) and C(25′), 0.24, and 0.24, respectively; for O(4) and O(4′), 0.38 and 0.24, respectively. For the THF, the site occupancy factors were determined using free variables. Anisotropic thermal parameters were refined for non-hydrogen atoms, except for the disordered atoms. Hydrogen atoms were placed at their calculated positions and refined using a riding model.

Table 2 Selected bond distances (Å) and angles (°) of compounds **1**, **2** and **4**[a]

	1	**2**	**4**
Fe(1)–O(1)	1.917(2)	1.910(2)	1.910(2)
Fe(1)–O(2)	1.916(2)	1.907(2)	1.914(2)
Fe(1)–O(3)	1.941(2)	1.901(2)	1.898(2)
Fe(1)–N(1)	2.223(2)	2.177(3)	2.143(2)
Fe(1)–N(2)	2.181(2)	2.193(3)	2.212(2)
Fe(1)–N(3)	2.202(2)	2.188(3)	2.172(2)
O(1)–Fe(1)–O(2)	98.2(1)	99.5(1)	98.6(1)
O(1)–Fe(1)–O(3)	95.6(1)	94.1(1)	95.0(1)
O(2)–Fe(1)–O(3)	99.3(1)	99.5(1)	97.7(1)
O(1)–Fe(1)–N(1)	83.7(1)	84.1(1)	84.6(1)
O(2)–Fe(1)–N(1)	92.3(1)	92.9(1)	95.7(1)
O(3)–Fe(1)–N(1)	168.4(1)	167.6(1)	166.5(1)
O(1)–Fe(1)–N(3)	91.9(1)	91.4(1)	92.4(1)
O(2)–Fe(1)–N(3)	168.2(1)	168.9(1)	168.4(1)
O(3)–Fe(1)–N(3)	85.5(1)	84.7(1)	85.0(1)
N(1)–Fe(1)–N(3)	82.9(1)	83.1(1)	81.5(1)
O(1)–Fe(1)–N(2)	169.9(1)	169.5(1)	172.0(1)
O(2)–Fe(1)–N(2)	84.1(1)	83.8(1)	83.6(1)
O(3)–Fe(1)–N(2)	93.7(1)	95.2(1)	92.3(1)
N(1)–Fe(1)–N(2)	86.4(1)	85.8(1)	87.6(1)
N(3)–Fe(1)–N(2)	84.9(1)	84.6(1)	85.0(1)

[a] Symmetry code A: for **1**, x, 0.5 − y, 1.5 − z; for **2**, x, 1.5 − y, 1.5 − z; for **3**, x, −0.5 − y, 1.5 − z; for **4**, 1 − x, y, 0.5 − z.

CCDC reference numbers 162677 (**1**), 194328 (**2**) and 194329 (**4**).

See http://www.rsc.org/suppdata/dt/b2/b209366a/ for crystallographic data in CIF or other electronic format.

Results and discussion

Synthesis and characterisation of 1

Reaction of $\mathbf{H_2L}$ with $Fe(NO_3)_3\cdot 9H_2O$ gives a dark-brown precipitate. Elemental analyses suggest the formation of triple-helical dinuclear compound. It seems that such a compound should contain iron ions with either +2 or +3 valence. In order to determine the valence of the iron ions, the temperature dependence of the molar magnetic susceptibility χ_m and the effective magnetic moment for a polycrystalline sample of the triple-helical compound **1** in the range of 75–300 K were carried out. The μ_{eff} *vs.* T plot for compound **1** is displayed in Fig. 1. The effective magnetic moment at room temperature of 6.82 μ_B, decreases slightly with decreasing temperature and reaches 6.23 μ_B, and the shapes of both curves are characteristic of very slightly antiferromagnetic coupling among the iron ions. It is proposed that the triple-helical iron complex con-

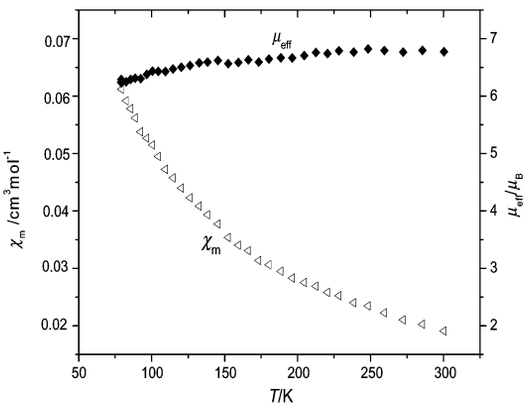

Fig. 1 Effective magnetic moment (μ_{eff}) and susceptibility χ_m data as a function of temperature for compound **1**.

tains two metal centers with uncoupling electrons. The effective magnetic moment at room temperature of 6.82 μ_B is also consistent with two high spin Fe^{II}.

Differential pulse voltammetry (DPV) technique is usually employed to obtain well-resolved potential information, while the individual redox processes for the multi-nuclear complexes are poorly resolved in the CV experiment, in which individual $E_{1/2}$ potentials cannot be easily or accurately extracted from this data.[26] In this technique, a working curve is used to convert the peak width at the half-height of the DPV peak into $\Delta E_{1/2}$ between the two closely spaced redox processes. Pulse voltammetry measurement of compound **1** (Fig. 2) exhibits three peaks at 0.775, 1.125 and 1.225 V. The peak corresponding to quinone oxidation appears at 0.775 V and the peaks corresponding to $E(Fe^{II}_2/Fe^{II}Fe^{III})$ and $E(Fe^{II}Fe^{III}/Fe^{III}_2)$ appear at 1.125 and 1.225 V, respectively. The separation between the potentials for the first and second steps is 0.100 V, indicating that there is no observable interaction between the Fe centers in this complex. The electron spectrum shows three broad bands at 360 nm (ε = 9800 M^{-1} cm^{-1}), 440 nm (ε = 2300 M^{-1} cm^{-1}) and 520 nm (ε = 1900 M^{-1} cm^{-1}), corresponding to the MLCT and d–d transitions, respectively.

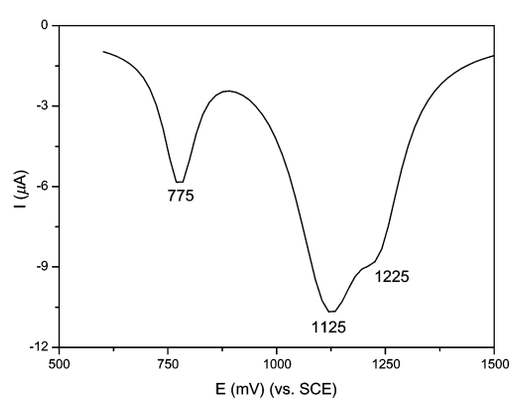

Fig. 2 Pulse voltammetry measurement of compound **1** in DMF solution containing 0.1 M tetrabutylammonium perchlorate as supporting electrolyte at a scan rate of 30 mV s^{-1}.

Crystal structure of 1

Crystallographic study of compound **1** has unequivocally confirmed the formation of the triple helical molecule (Fig. 3). Compound **1** crystallizes in a centrosymmetric space group *Pnna*, consequently the molecules occur as a racemic mixture of Δ–Δ and Λ–Λ configuration enantiomers, whereby the equivalent fragments are inter-related by the C_2 axis which runs perpendicularly to the N(3)–N(3A) (symmetry code A: x, 0.5 − y, 1.5 − z) line (Fig. 3). Each iron center is bound to three ON

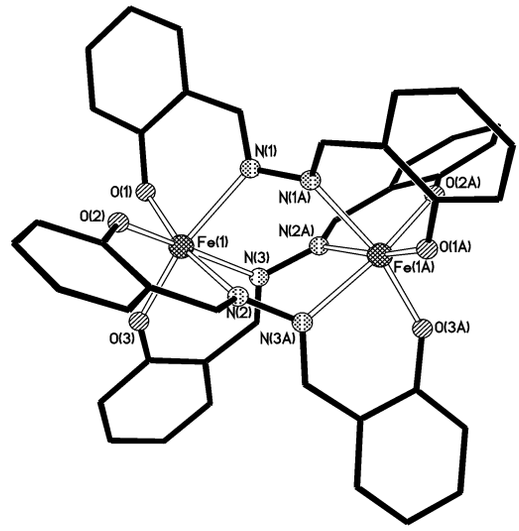

Fig. 3 Molecular structure of the triple helical compound **1**. Symmetry code A: x, 0.5 − y, 1.5 − z.

binding units to attain a distorted octahedral coordination geometry with Fe ··· Fe separation of *ca.* 3.99 Å. Each ligand loses protons and coordinates to two metal centers as a bis(bidentate) ligand to form a helical complex. Bond distances and angles are in the normal ranges. Coordination to the metal center forces inter-planar twisting between the two phenyl rings of each ligand, the dihedral angle is *ca.* 36° between phenyl rings III and IIIA, and *ca.* 56° between phenyl rings I and IIA, where phenyl ring I, II and III are defined by the carbon atoms C(1) to C(6), C(8) to C(13) and C(15) to C(20).

The most distinctive structural feature of the compound in the solid state is that it forms a two-dimensional channeled framework (Fig. 4) and the diethyl ether molecules are adsorbed in the channels. The intermolecular π–π interactions which linked the phenyl rings I and IIIB, III and IC (symmetry code B: −x, 0.5 + y, 0.5 + z; C: x, 1 − y, 2 − z) into a one-dimensional chain are quite similar to the P4PE (parallel four fold phenyl embrace) motif described by Scudder and Dance[10] for tetraphenylphosphonium cations in which two of the four phenyl rings [I and IC] are parallel and the motif comprises one offset face-to-face attractive interaction and two edge-to-face C–H ··· π interactions. The π–π stacking interaction between parallel aromatic rings I and IC is characterized by the shortest inter-planar atom ··· atom separation [C(5) ··· C(5C)] of 3.45 Å. The C–H ··· π interactions are characterized by the H ··· M distance of 2.89 Å (M being the midpoint of the phenyl ring IIIC), with a C–H ··· M angle [C(4)–H(4A) ··· M] of 134°. The phenyl ring II is stacked with the symmetry related one IID (symmetry code D: 0.5 − x, −y, z)

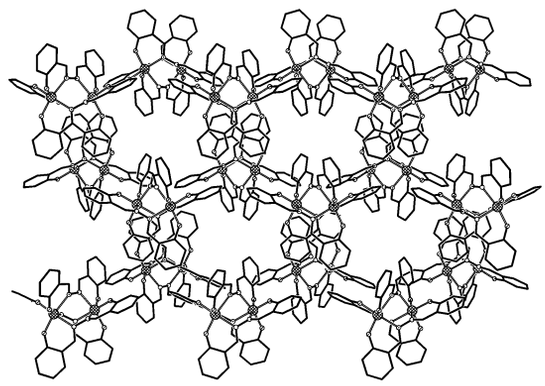

Fig. 4 View of the two-dimensional channel structure in compound **1** showing intermolecular π–π stacking interactions and C–H ··· π interactions between the phenyl rings. Hydrogen atoms are omitted for clarity.

to complete the two-dimensional brick-wall like sheet of hexagons. The members of the stacking pair are parallel to each other with the shortest inter-planer center–center separation of 3.74 Å. At the same time, there is also a C–H ··· π interaction between the carbon atom C(10) and the phenyl ring IIIE (symmetry code E: 1.5 − *x*, *y*, 2 − *z*) in the same sheet with the H ··· M′ (midpoint of the phenyl ring IIIE) of 2.87 Å and C–H ··· M angle [C(10)–H(10A) ··· M′] of 156°, respectively. These results suggested that interconnected systems of aromatic ··· aromatic interactions possess the property of being co-operative, that is the contacts enhance the strength of each other, and the interaction energy per contact is greater than the energy of an isolated interaction. Those two-dimensional sheets are packed parallel each other in the crystal to form the channeled structure, and one diethyl ether molecule per molecule is filled in the channels. The shortest intermolecular atom ··· atom separation between the host and the diethyl ether guest molecule is 3.58 Å [C(2) ··· C(25)], indicating weak Van der Waals interactions between the host and guest molecules exist to stabilize the inclusion compound. It is also interesting to note that π–π (face-to-face) and C–H ··· π interactions link molecules of the triple-helical $\mathbf{Fe_2L_3}$ into two-dimensional channel frame-works, while molecules in the structural related complex $\mathbf{Fe_2L'_3}$ are linked into a three-dimensional porous framework,[16] and guest molecules are adsorbed in the porous framework. It is suggested that the existence of hydrogen bonds related to the hydroxyl groups in the $\mathbf{Fe_2L'_3}$ molecules is the important factor influencing the crystal packing.

Crystal structure of 2

The aim of crystal engineering is to establish reliable connections between molecular and supramolecular structure on the basis of intermolecular interactions. Ideally, one would like to identify substructural units in a target supramolecule that can be assembled from logically chosen precursor. Therefore the predictable self-organization of molecules into one-, two- or three-dimensional networks are of importance in crystal engineering. For such rational design, intermolecular interactions, be they strong or not so strong, are significant enough in combination that the orientation of molecules in the solid can be predicted with a reasonable degree of accuracy. To this end, the triple helical molecule $\mathbf{Fe_2L_3}$ was recrystallized in pyridine solvent to give crystal **2**. It is interesting to find that crystals **2** and **1** are isostructual features both in molecular structure and space group, in which similar channeled framework was formed. The only difference is that the included guests are pyridine for crystal **2** and diethyl ether for crystal **1**. Like that of compound **1**, the phenyl rings I, IIIB, IC and III (symmetry code B: −*x*, −0.5 + *y*, 0.5 + *z*, C: −*x*, 1 − *y*, 1 − *z*) compose a similar P4PE motif through which molecules are held into a one-dimensional chain. The π–π stacking interaction between parallel aromatic rings I and IC is characterized by a shortest inter-planar atom ··· atom separation [C(5) ··· C(5C)] of 3.39 Å. The C–H ··· π interactions are characterized by the H ··· M (midpoint of the phenyl ring IIIB) of 2.91 Å, with C–H ··· M angle [C(4)–H(4A) ··· M] of 128°. The phenyl ring II is stacked with the symmetry related one IID to complete the brick-wall like two-dimensional sheet with hexagons (symmetry code D: −0.5 − *x*, 2 − *y*, *z*). The members of the stacking pair are parallel to each other with the shortest inter-planer atom ··· atom separation of 3.55 Å and the center ··· center separation of 3.59 Å. There is also a C–H ··· π interaction between the carbon atom C(10) and the phenyl ring IIIE (symmetry code E: −0.5 − *x*, 1 − *y*, 1 − *z*) in the same sheet with the H ··· M′ (midpoint of the phenyl ring IIIE) of 2.95 Å and C–H ··· M angle [C(10)–H(10A) ··· M′] of 156°, respectively. Weak Van der Waals interactions between the host and guest molecules are also found to stabilize the inclusion compound, since the shortest intermolecular atom ··· atom separation between the host and the diethyl ether guest molecule is 3.47 Å [C(9) ··· C(23)]. Since the cell parameters of compound **3** are quite similar to those of compound **2**, intensities of compound **3** were not measured completely, however, it should be expected that such a crystal structure is almost the same to that of compound **2** both in the molecular structure and crystal-packing pattern.

Crystal structure of 4

Although not crystallized in the space group *Pnna* like that of compounds **1**, **2** and **3**, molecules of compound **4** also occur as racemic mixture of a Δ–Δ and Λ–Λ configuration enantiomers, whereby the equivalent fragments are inter-related by the C_2 axis which runs perpendicularly to the N(3)–N(3A) (symmetry code A: 1 − *x*, *y*, 0.5 − *z*) line. Each iron center is bound to three ON binding units to attain a distorted octahedral coordination geometry with an Fe ··· Fe separation of *ca.* 3.96 Å. Each ligand loses protons and coordinates to two metal centers as a bis(bidentate) ligand to complex the helical arrangement. Bond distances and angles are in the normal ranges. Detailed crystal structure analyses (Fig. 5) indicate that the phenyl ring III is stacked with the symmetry related phenyl rings IIIB (symmetry code B: 1 − *x*, −*y*, −*z*) with the shortest inter-planar atom ··· atom separation [C(17) ··· C(19B)] of 3.47 Å to form a one-dimensional chain. Each chain connects the adjacent ones using C–H ··· π interaction with the type C(10)–H(10A) ··· M (M is the center of the phenyl ring IIIC symmetry code C: 1.5 − *x*, 0.5 + *y*, *z*) to construct the two-dimensional sheet, the H ··· M′ is 3.05 Å and C–H ··· M′ angle is 148°, respectively. Those two-dimensional sheets are further packed parallel each other in the crystal to form the channeled structure, and four THF molecules per molecular are filled in the channels.

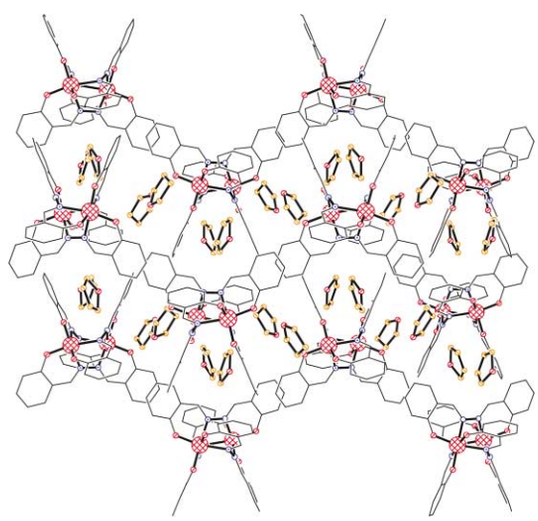

Fig. 5 View of the two-dimensional channel structure in compound **4**.

Thermogravimetric analyses

The most important factor in seeking and developing new molecular-based porous materials is whether the frameworks of such materials are stable even after removal of guest molecules.[27] As we know, many porous systems, upon removal of the included guest molecules, often undergo phase transitions to other more dense structures.[28,29] To study the inclusion chemistry of these materials, thermogravimetric analysis (TGA) was performed on a crystalline sample of compound **1**, which showed the following strikingly clean and well-separated weight loss steps (Fig. 6). An initial weight loss of 8.4% about 220 °C corresponds to the removal of one diethyl ether per formula unit (calc. 8.2%). More significant thing is that all the diethyl ether guests can be evacuated from the pores within the temper-

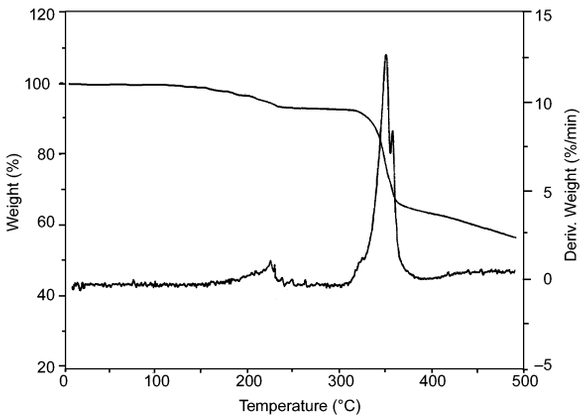

Fig. 6 DTA and TGA for compound **1** from 25 to 500 °C.

ature range of 220–320 °C, without loss of the framework periodicity. In addition, the desolvated compound **5** was checked by elemental microanalysis. The stability of this network was studied by X-ray powder diffraction (XRPD) with a simulated pattern based on the single crystal data (Fig. 7). It seems that the porous network is retained in this phase in the absence of any guest molecules in the cavities, however, it is also seen that the evacuation of the guest could cause small changes in the cell dimensions (Table 3). Thermogravimetric analyses of the crystalline samples **2**, **3** and **4** were also studied for comparison. As shown in Fig. 8, strikingly clean and well-separated weight loss steps were observed: an initial weight loss corresponds to the removal of guest molecules about 100 °C or higher temperature, and all the guests can be evacuated from the pores within the temperature range of 220–320 °C, without loss of the framework periodicity.

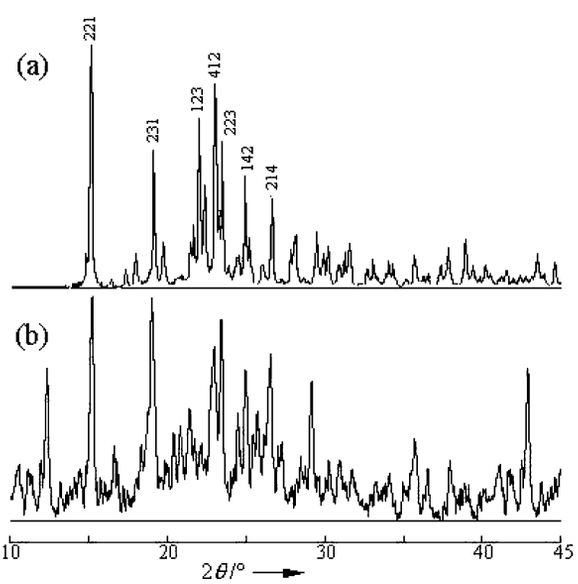

Fig. 7 X-Ray powder diffraction pattern for compounds **1** and **5**; (a) calculated from the single-crystal data of compound **1**; (b) the X-ray powder diffraction of compound **5**.

Furthermore, solid **6** was obtained by adding solid **5** to a diethyl ether solution. Elemental microanalysis and thermogravimetric analysis (Fig. 9a) for the re-absorbed materials confirm the presence of diethyl ether guests. Also, there is no obvious difference in either their morphologies or crystallinities as evidenced by another X-ray powder diffraction study (Table 3), and the cell dimensions calculated from the powder diffractions clearly indicate that the the cell dimensions of compound **6** are more close to compound **1** than those of compound **5**. Presumably, the triple-helical frameworks are preserved throughout the cycle of heating, cooling and inclusion. Solids **7** and **8** were obtained by adding solid **5** to *n*-hexane and cyclohexane solutions, respectively. It is interesting to find that thermal gravimetric measurement and elemental microanalysis (Fig. 9b and c) do not support the absorbance of any guest, indicating that the inclusion can be selectively re-absorbed.

Table 3 The *d* spacings and indexes of compounds **5** and **6** from X-ray powder diffraction and single crystal analyses of compound **1**

Compound **1**		Compound **5**		Compound **6**	
a = 19.446(4) Å b = 16.670(3) Å c = 14.582(3) Å V = 4727(2) Å^3		a = 19.35 Å b = 16.91 Å c = 14.47 Å V = 4734 Å^3		a = 19.42 Å b = 16.79 Å c = 14.55 Å V = 4744 Å^3	
d_{calc}	$h\,k\,l$	d_{obs}	d_{calc}	d_{obs}	d_{calc}
5.80	221	5.81	5.83	5.82	5.82
4.58	231	4.66	4.62	4.65	4.60
4.11	123	4.14	4.10	4.16	4.11
3.93	412	3.87	3.91	3.90	3.93
3.86	223	3.79	3.84	3.80	3.85
3.56	142	3.56	3.58	3.55	3.57
3.35	214	3.36	3.32	3.37	3.34
		Standard dev.[a] 0.01		Standard dev.[a] 0.01	

[a] Standard dev. = $|(d_{obs} - d_{calc})|/d_{calc}$.

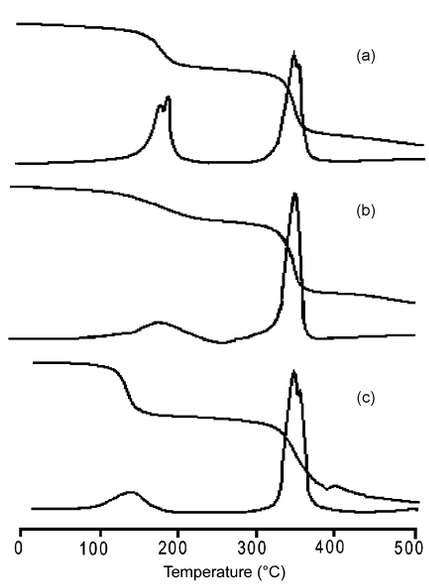

Fig. 8 Thermal properties of compounds **2**–**4** ranging from 25 to 500 °C; (a) DTA and TGA for compound **2**; (b) DTA and TGA for compound **3**; (c) DTA and TGA for compound **4**.

The facility with which the volatile small molecules inclusion occurs, coupled with the fact that the morphology of its crystalline particles is retained throughout the inclusion processes, is further evidence that the volatile molecules are diffused into the framework without any destruction of the host network. This fact, the absence of counter ions, and the significant thermal stability, make these and related materials exciting new candidates for examination of their potential utility in, for example, catalysis or separation processes. It is also noted that although the energies of the C–H $\cdots$ π interactions are only 2–20 kJ mol^{-1},[22] their effects on crystal structure and packing are as predictable as those of conventional hydrogen bonding and strong stacking interactions. This kind of non-covalent interaction has the potential to assemble smaller or simpler fragments into the desired cavities under favorable conditions, which is important in host–guest chemistry and has applications in chemistry, biology and materials science.

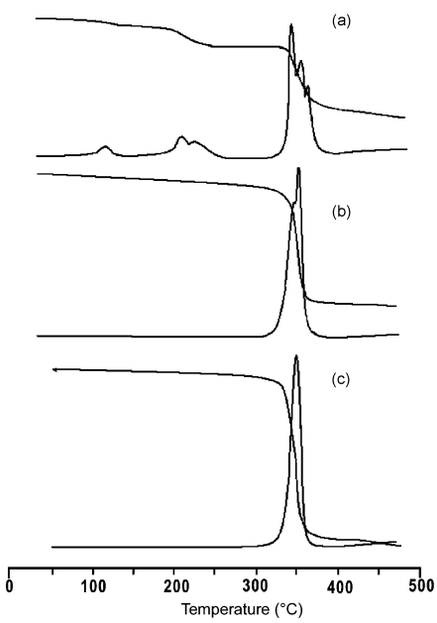

Fig. 9 Thermal properties of compounds **6**–**8** ranging from 25 to 500 °C; (a) DTA and TGA for compound **6**; (b) DTA and TGA for compound **7**; (c) DTA and TGA for compound **8**.

Acknowledgements

This work is supported by the National Natural Science Foundation of China. We thank Mr. Liu Yong-jiang for collecting the single crystal data and Mr. Ye Yu-da for providing the powder X-ray diffraction measurements.

References

1 (*a*) C. A. Hunter, *Chem. Soc. Rev.*, 1994, 101; (*b*) C. A. Hunter, *J. Mol. Biol.*, 1993, **230**, 1025; (*c*) C. A. Hunter, *J. Am. Chem. Soc.*, 1992, **114**, 5303; (*d*) F. J. Carver, C. A. Hunter, D. J. Livingstone, J. F. McCabe and E. M. Sewardet, *Chem. Eur. J.*, 2002, **8**, 2848.

2 (*a*) G. R. Desiraju, *Crystal Engineering: The Design of Organic Solids*, Elsevier, Amsterdam, 1989; (*b*) G. R. Desiraju, *Angew. Chem., Int. Ed. Engl.*, 1995, **34**, 2311; (*c*) G. R. Desiraju, *Chem. Commun.*, 1997, 1475.

3 (*a*) D. Philp and J. F. Stoddart, *Angew. Chem., Int. Ed. Engl.*, 1996, **35**, 1154; (*b*) P. L. Anelli, P. R. Ashton, R. Ballardini, V. Balzani, M. Delgado, M. T. Gandolfi, A. E. Kaifer, D. Philp, M. Pietraszkiewicz, L. Prodi, M. V. Reddington, A. M. Z. Slawin, N. Spencer, J. F. Stoddart, C. Vicent and D. J. Williams, *J. Am. Chem. Soc.*, 1992, **114**, 193.

4 (*a*) K. Biradha and M. J. Zaworotko, *J. Am. Chem. Soc.*, 1998, **120**, 6431; (*b*) W. L. Jorgensen and D. L. Severance, *J. Am. Chem. Soc.*, 1990, **112**, 4768.

5 (*a*) G. R. Desiraju and A. Gavezzotti, *J. Chem. Soc., Chem. Commun.*, 1989, 621; (*b*) P. M. Zorky and O. N. Zrukya, *Adv. Mol. Struct. Res.*, 1993, **3**, 147.

6 (*a*) G. R. Desiraju, *Chem. Mater.*, 1994, **6**, 1282; (*b*) N. N. L. Madhavi, A. K. Katz, H. L. Carrell, A. Nangia and G. R. Desiraju, *Chem. Commun.*, 1997, 1953; (*c*) H. C. Weiss, D. Bläser, R. Boese, B. M. Doughan and M. M. Haley, *Chem. Commun.*, 1997, 1703.

7 (*a*) K. N. Houk, S. Menzer, S. P. Newton, F. M. Raymo, J. F. Stoddart and D. J. Williams, *J. Am. Chem. Soc.*, 1999, **121**, 1479; (*b*) M. Asakawa, P. P. Ashton, S. E. Boyd, C. L. Brown, S. Menser, D. Pasini, J. F. Stoddart, M. S. Tolley, A. T. P. White, D. J. Williams and P. G. Wyah, *Chem. Eur. J.*, 1997, **3**, 463.

8 (*a*) C. A. Hunter and J. K. M. Sanders, *J. Am. Chem. Soc.*, 1990, **112**, 5525; (*b*) J. Zhang and J. S. Moore, *J. Am. Chem. Soc.*, 1992, **114**, 9701; (*c*) J. E. Kickham, S. J. Loeb and S. L. Murphy, *J. Am. Chem. Soc.*, 1993, **115**, 7031.

9 (*a*) C. J. Fang, C. Y. Duan, C. He, G. Han and Q. J. Meng, *New J. Chem.*, 2000, **24**, 697; (*b*) Z. H. Liu, C. Y. Duan, J. H. Li, Y. J. Liu, Y. H. Mei and X. Z. You, *New J. Chem.*, 2000, **24**, 1057; (*c*) Z. H. Liu, C. Y. Duan, J. Hu and X. Z. You, *Inorg. Chem.*, 1999, **38**, 1719.

10 (*a*) I. Dance and M. Scudder, *Chem. Eur. J.*, 1996, **2**, 481; (*b*) I. Dance and M. Scudder, *J. Chem. Soc., Chem. Commun.*, 1995, 1039; (*c*) I. Dance and M. Scudder, *J. Chem. Soc., Dalton Trans.*, 1998, 1341; I. Dance and M. Scudder, *J. Chem. Soc., Dalton Trans.*, 1996, 3755; (*d*) M. Scudder and I. Dance, *J. Chem. Soc., Dalton Trans.*, 1998, 329; M. Scudder and I. Dance, *J. Chem. Soc., Dalton Trans.*, 1998, 3167; (*e*) C. Hasselgren, P. A. W. Dean, M. L. Scudder, D. C. Craig and I. Dance, *J. Chem. Soc., Dalton Trans.*, 1997, 2019.

11 (*a*) W. Saengew, *Principles of nucleic acid structures*, Springer-Verlag, New York, 1984, pp. 132–140; (*b*) S. O. Kelley, R. E. Holmlin, E. D. A. Stemp and J. K. Barton, *J. Am. Chem. Soc.*, 1997, **119**, 9861; (*c*) M. R. Arkin, E. D. A. Stemp, R. E. Holmlin, J. K. Barton, A. Hormann, E. J. C. Olson and P. A. Barbara, *Science*, 1996, **273**, 475.

12 (*a*) M. Bastian and H. Sigel, *Inorg. Chem.*, 1997, **36**, 1619; (*b*) T. Sugimori, H. Masuda, N. Ohata, K. Koiwai, A. Odani and O. Yamauchi, *Inorg. Chem.*, 1997, **36**, 576; (*c*) E. Kim, S. Paliwal and C. S. Wilcox, *J. Am. Chem. Soc.*, 1998, **120**, 11192.

13 (*a*) D. J. Cram, *Angew. Chem., Int. Ed. Engl.*, 1988, **27**, 1009; (*b*) R. J. Jansen, A. E. Rowan, R. de. Gelder, H. W. Scheeren and R. J. M. Nolte, *Chem. Commun.*, 1998, 121.

14 (*a*) B. Gong, C. Zheng, H. Zeng and J. Zhu, *J. Am. Chem. Soc.*, 1999, **121**, 9766; (*b*) M. J. Cloninger and H. W. Whitlock, *J. Org. Chem.*, 1998, **63**, 6153.

15 (*a*) V. R. Thalladi, S. Brasselet, H.-C. Weiss, D. Bläser, A. K. Katz, H. L. Carrell, R. Boese, J. Zyss, A. Nangia and G. R. Desiraju, *J. Am. Chem. Soc.*, 1998, **120**, 2563; (*b*) J. A. Swift, R. Pal and J. M. McBride, *J. Am. Chem. Soc.*, 1998, **120**, 96; (*c*) J. A. Swift, V. A. Russel and M. D. Ward, *Adv. Mater.*, 1997, **9**, 1183; (*d*) V. R. Thalladi, R. Boese, S. Brasselet, I. Ledoux, J. Zyss, R. K. R. Jetti and G. R. Desiraju, *Chem. Commun.*, 1999, 1639.

16 H. Mo, D. Guo, C. Y. Duan, Y. T. Li and Q. J. Meng, *J. Chem. Soc., Dalton Trans.*, 2002, 3422.

17 (*a*) P. K. Bowyer, K. A. Porter, A. D. Rae, A. C. Willis and S. B. Wild, *Chem. Commun.*, 1998, 1153; (*b*) M. J. Hannon, C. L. Painting and N. W. Alcock, *Chem. Commun.*, 1999, 2023; (*c*) M. J. Hannon, S. Bunce, A. J. Clarke and N. W. Alcock, *Angew. Chem., Int. Ed.*, 1999, **38**, 1277; (*d*) A. Ziessel, A. Harriman, A. El-Ghayoury, L. Douce, E. Leize, H. Nierengarten and A. V. Dorsselaer, *New J. Chem.*, 2000, **24**, 729.

18 (*a*) D. Guo, C. He, C. Y. Duan, C. Q. Qian and Q. J. Meng, *New J. Chem.*, 2002, **26**, 796; (*b*) D. Guo, C. Y. Duan, C. J. Fang and Q. J. Meng, *J. Chem. Soc., Dalton Trans.*, 2002, 834; (*c*) G. Hang, D. Guo, C. Y. Duan, H. Mo and Q. J. Meng, *New J. Chem.*, 2002, **26**, 1371.

19 (*a*) S. C. Zimmerman, *Science*, 1997, **276**, 543; (*b*) A. Gavezzotti, *Acc. Chem. Res.*, 1994, **27**, 309; (*c*) V. A. Russell, C. C. Evans, W. Li and M. D. Ward, *Science*, 1997, **276**, 575.

20 (*a*) G. M. J. Schmidt, *Pure Appl. Chem.*, 1971, **27**, 647; (*b*) J. D. Dunitz, *Pure Appl. Chem.*, 1991, **63**, 177; (*c*) D. Venkataraman, S. Lee, J. Zhang and J. S. Moore, *Nature*, 1994, **371**, 591.

21 (*a*) V. A. Russell and M. D. Ward, *Chem. Mater.*, 1996, **8**, 1684; (*b*) V. A. Russell, M. C. Etter and M. D. Ward, *J. Am. Chem. Soc.*, 1994, **116**, 1941; (*c*) S. V. Kolotuchin, E. E. Fenlon, S. R. Wilson, C. J. Loweth and S. C. Zimmerman, *Angew. Chem., Int. Ed. Engl.*, 1995, **34**, 2654; (*d*) M. D. Hollingsworth, M. E. Brown, A. C. Hillier, B. D. Santarsiero and J. D. Chaney, *Science*, 1996, **273**, 1355.

22 (*a*) T. Steiner, E. B. Starikov and M. Tamm, *J. Chem. Soc., Perkin Trans. 2*, 1996, 67; (*b*) T. Steiner, E. B. Starikov, A. M. Amado and J. J. C. T. Teixeira-Dias, *J. Chem. Soc., Perkin Trans. 2*, 1995, 1321.

23 SMART and SAINT, Area Detector Control and Integration Software, Siemens Analytical X-Ray Systems, Inc., Madison, WI, USA, 1996.

24 XSCANS, Siemens Analytical X-ray Instruments, Inc., Madison, WI, USA, ver. 2.1, 1994.

25 G. M. Sheldrick, SHELXTL V5.1 Software Reference Manual, Bruker AXS, Inc., Madison, WI, USA, 1997.

26 (*a*) R. S. Barbara, A. A. Kevin, C. M. Elliott and O. P. Anderson, *Inorg. Chem.*, 1988, **27**, 4499; (*b*) D. E. Richardson and H. Taube, *Inorg. Chem.*, 1981, **20**, 1278.

27 (*a*) G. B. Gardner, Y.-H. Kiang, S. Lee, A. Asgaonkar and D. Venkataraman, *J. Am. Chem. Soc.*, 1996, **118**, 6946; (*b*) S. Kitagawa and M. Kondo, *Bull. Chem. Soc. Jpn.*, 1998, **71**, 1739.

28 X. Wang, M. Simard and J. D. Wuest, *J. Am. Chem. Soc.*, 1994, **116**, 12119.

29 (*a*) B. F. Hoskins and R. Robson, *J. Am. Chem. Soc.*, 1990, **112**, 1546; (*b*) B. F. Abrahams, B. F. Hoskins, D. M. Michail and R. Robson, *Nature*, 1994, **369**, 727.